

MM Science Journal | www.mmscience.eu

ISSN 1803-1269 (Print) | ISSN 1805-0476 (On-line)

Special Issue | HSM 2025

18th International Conference on High Speed Machining October 15-16, 2025, Metz, France

DOI: 10.17973/MMSJ.2025_11_2025128



HSM2025-44707

ENHANCING PRODUCTIVITY AND SUSTAINABILITY IN MANUFACTURING THROUGH DYNAMIC CONTROL OF 5-AXIS CONICAL TAPER BARREL MACHINING OPERATIONS

R. Bonnell¹, R. Carroll¹, C. Green¹, A. Brown¹, R. Ward^{2*}

¹University of Sheffield Advanced Manufacturing Research Centre, Rotherham, UK

²University of Sheffield, School of Electrical and Electronic Engineering, Sheffield, UK

*Corresponding author; e-mail: r.a.ward@sheffield.ac.uk

Abstract

The machining industry aims to boost productivity and sustainability through advanced machining strategies like conical taper barrel milling. These tools, with large contact radii, enhance surface quality, efficiency, and material removal on freeform surfaces. However, industry uptake is limited by challenges in programming varying tilt angles leading to uneven tool wear. Unlike lathes using G96 to maintain constant surface speed, milling machines use fixed spindle speeds, making them less adaptable. This paper presents a novel method for 5-axis control of conical taper barrel tools by dynamically adjusting spindle speed, feedrate, TCP position, and tool orientation. Machining trials validate the method's effectiveness.

Keywords

Conical Taper Barrell Milling, 5-Axis Milling, Variable Spindle Speed Control

1 INTRODUCTION

The requirement for higher productivity and sustainability in machining has driven the development of advanced tool geometries and machining strategies. Among these, barrel milling tools, particularly conical taper barrel (CTB) cutters have gained attention for their ability to enhance surface quality and material removal rates in freeform surface machining [Lu et al. 2019; Luo et al. 2016]. These tools leverage larger effective cutting radii, allowing for increased stepover distances while maintaining cusp height, thereby improving machining efficiency.

CTB geometry milling tools are becoming more prevalent in subtractive manufacturing as CAM and simulation software increase in their functionality and develop new technologies to support their use. Typical commodities that benefit from the application of CTB's include aeroengine blisk / blade type features and medical femoral knee implants, which both have freeform concave/convex surfaces in common. This type of surface lends itself to machining with a CTB tool but poses challenges in terms of the tool tangency contact point and maintaining a constant surface speed (Vc) and chip thickness (h) when this point varies. This is particularly relevant to critical features as any variance in machining parameters can have a direct effect on the component's performance and service life.

In femoral knee implant manufacture, there is currently a significant push towards replacing the incumbent grinding process of the condyle surface with a defined edge subtractive process. The work detailed in this paper has the potential to lead to additional benefits, supporting the move to this new process through productivity increases and extended tool life.

Despite their advantages, the adoption of conical taper barrel milling in industry has been limited due to challenges in tool path programming and process control. Traditional milling operations rely on fixed spindle speeds and tool diameters, unlike turning operations where constant surface speed (CSS) control (e.g., G96 in ISO 6983) dynamically adjusts rotational speed to maintain optimal cutting conditions. The variable cutting diameter of conical taper barrel tools necessitates similar adaptive control strategies to maintain consistent chip load and surface speed, yet conventional CNC milling systems lack built-in functionality for such adjustments.

Recent research [Vavruska et al. 2023] has explored methods to optimise tool orientation and cutting parameters for barrel milling tools. For instance, (Meng et al., 2014) proposed a method for optimal barrel cutter selection for blisk machining, considering geometric properties, tool rigidity, and machine kinematic constraints to enhance productivity. [Reznicek et al. 2025] investigated the impact of barrel cutter radius and machining parameters on cutting forces and surface roughness during the milling of spherical surfaces, noting that smaller-radius tools and internal geometries are preferable for minimising forces. Additionally, [Jiang et al. 2024] introduced a novel "barreltaper-ball milling cutter" and a corresponding cutting dynamics model, demonstrating that it can significantly increase the cutting step for the same surface roughness, thereby reducing processing time.

Dynamic spindle speed modulation (DSSM) and feedrate adaptation have been successfully applied in conventional milling to improve machining stability and tool life, but their

extension to variable-diameter tools remains underexplored.

The integration of 5-axis machining further complicates control strategies, as tool centre point (TCP) positioning and orientation must be synchronised with spindle speed and feedrate adjustments. While some studies have proposed offline compensation methods for barrel milling [Suzuki et al. 2021], a real-time adaptive control approach, akin to CSS in turning, has not yet been fully realised for conical taper barrel tools. This gap highlights the need for a systematic method to dynamically regulate machining parameters in response to the tool's varying engagement conditions

This paper addresses this challenge by introducing a novel control strategy for conical taper barrel milling that dynamically adjusts spindle speed, feedrate, TCP position, and tool orientation. The proposed method bridges the gap between traditional fixed-diameter milling and adaptive turning strategies, offering a pathway toward more efficient and sustainable machining of complex surfaces. The paper also highlights the practical challenges and limitations faced during implementation of the proposed method.

The paper is structured as follows, section 2 presents the methodology, section 3 experimental trials, section 4 results and concludes with section 5.

2 METHODOLOGY

The section presents the development of the proposed method.

If the contact point of the barrel mill (as seen in Figure 1) with the part surface is programmed to continuously roll down (or up) the large barrel radius then to maintain a constant surface speed and feed per tooth (or maximum chip thickness) between the cutting tool and the part surface will necessitate a line-by-line updating of the spindle speed and feedrate in the NC code.

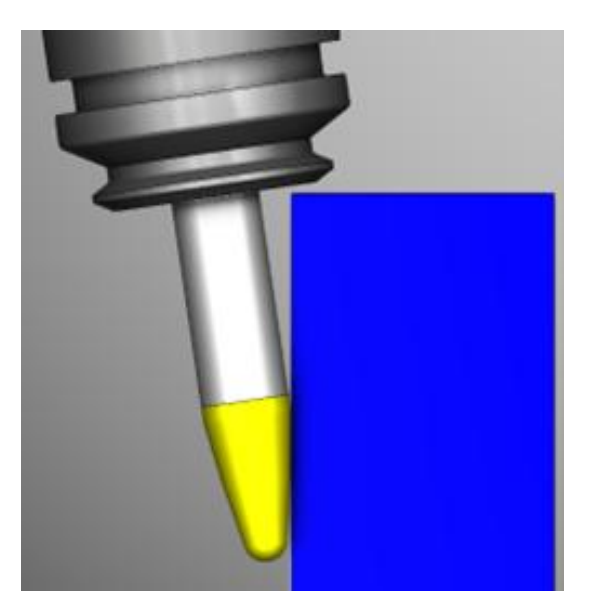


Fig. 1: CTB milling tool in contact with workpiece

For example, as shown in Figure 2, a toolpath with the contact point rolling down the nominal conical barrel mill tool shown below from the top point at 15mm effective diameter to the bottom point at 6mm effective diameter would have to smoothly adapt the spindle speed of the cutting tool from 2122RPM up to 5305RPM to maintain a constant surface speed of 100m/min.

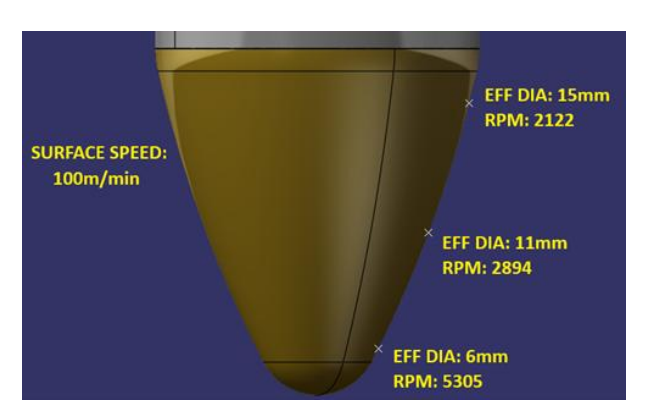


Fig. 2: RPM variation with contact point to maintain a constant surface speed..

To enable the varying spindle speed and feed to be calculated in the post processor the following parameters must be output in the cutter location (CL) data at every point in the tool path at which the cutting tool is in contact with the material:

- The X, Y and Z axis values of the tool centre point. (Tx, Ty, Tz)
- The I, J and K values that are the components of the tool axis vector. (i, j, k)
- The X, Y and Z axis values of the contact point between the tool and the material. (Cx, Cy, Cz)

These values are all output relative to the active workpiece coordinate system (WCS). The constant surface speed operations were programmed in CATIA v5-6 R2024, outputting 12 parameter GOTO lines, which included these 9 parameters in addition to the 3 surface normal vector components.

An example of this output is shown here:.

GOTO / 52.955656070, 119.648085095, 1.305799988, 0.265367681,0.938981311, -0.218847189, 52.955656,119.648085, 1.305800,0.207911691, 0.978147601, 0.000000000

Though the calculation would be more straightforward when using all 12 of these parameters, only the first 9 of these parameters were used by the AMRC's Post Processor to provide forward compatibility for potential future applications with the 9-parameter output from Siemens NX.

With these 9 values the effective diameter can be calculated using vector algebra as follows. Using X, Y, Z values of both the tool centre point, T, and the contact point, C create the vector TC. Taking the magnitude of the cross product of the tool vector axis vector, v, with the vector TC gives the area of the parallelogram formed from the two vectors, shown in Figure 3.

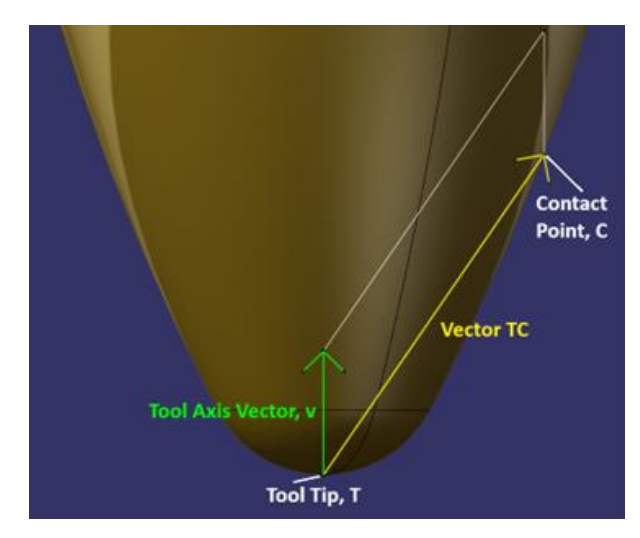


Fig. 3: Parallelogram whose area is found by taking the cross product of the vectors.

As the area of a parallelogram is its base multiplied by its vertical height, we can take the tool axis vector to be its base and so the vertical height will be the distance from the contact point to the tool axis, the effective radius of the cutting tool.

As the tool axis vector supplied in the APTSource file is a unit vector, then this effective radius will equal the area of the parallelogram and the effective diameter, D_{eff} , at this contact point will be:

$$D_{eff} = 2\|\mathbf{v} \times \mathbf{T}\mathbf{C}\| = 2 \left\| \begin{pmatrix} i \\ j \\ k \end{pmatrix} \times \begin{pmatrix} C_{x} - T_{x} \\ C_{y} - T_{y} \\ C_{z} - T_{z} \end{pmatrix} \right\| = 2 \left\| \begin{pmatrix} i \\ j \\ k \end{pmatrix} \times \begin{pmatrix} C_{x} - T_{x} \\ C_{y} - T_{y} \\ C_{z} - T_{z} \end{pmatrix} \right\| = 2 \left\| \begin{pmatrix} (C_{x} - T_{x})k - (C_{y} - T_{y})k \\ (C_{y} - T_{y})i - (C_{x} - T_{x})j \\ + ((C_{x} - T_{x})k - (C_{z} - T_{z})i)^{2} + \cdots + ((C_{y} - T_{y})i - (C_{x} - T_{x})j)^{2} + \cdots + ((C_{y} - T_{y})i - (C_{x} - T_{x})j)^{2} + \cdots + ((C_{y} - T_{y})i - (C_{x} - T_{x})j)^{2} + \cdots + ((C_{y} - T_{y})i - (C_{x} - T_{x})j)^{2} + \cdots + ((C_{y} - T_{y})i - (C_{x} - T_{x})j)^{2} + \cdots + ((C_{y} - T_{y})i - (C_{x} - T_{x})j)^{2} + \cdots + ((C_{y} - T_{y})i - (C_{x} - T_{x})j)^{2} + \cdots + ((C_{y} - T_{y})i - (C_{x} - T_{x})j)^{2} + \cdots + ((C_{y} - T_{y})i - (C_{x} - T_{x})j)^{2} + \cdots + ((C_{y} - T_{y})i - (C_{x} - T_{x})j)^{2} + \cdots + ((C_{y} - T_{y})i - (C_{x} - T_{x})j)^{2} + \cdots + ((C_{y} - T_{y})i - (C_{x} - T_{x})j)^{2} + \cdots + ((C_{y} - T_{y})i - (C_{x} - T_{x})j)^{2} + \cdots + ((C_{y} - T_{y})i - (C_{y} - T_{y})i - (C_{y} - T_{y})j)^{2} + \cdots + ((C_{y} - T_{y})i - (C_{y} - T_{y})i - (C_{y} - T_{y})j)^{2} + \cdots + ((C_{y} - T_{y})i - (C_{y} - T_{y})i - (C_{y} - T_{y})j)^{2} + \cdots + ((C_{y} - T_{y})i - (C_{y} - T_{y})j)^{2} + \cdots + ((C_{y} - T_{y})i - (C_{y} - T_{y})j)^{2} + \cdots + ((C_{y} - T_{y})i - (C_{y} - T_{y})j)^{2} + \cdots + ((C_{y} - T_{y})i - (C_{y} - T_{y})j)^{2} + \cdots + ((C_{y} - T_{y})i - (C_{y} - T_{y})j)^{2} + \cdots + ((C_{y} - T_{y})i - (C_{y} - T_{y})j)^{2} + \cdots + ((C_{y} - T_{y})i - (C_{y} - T_{y})j)^{2} + \cdots + ((C_{y} - T_{y})i - (C_{y} - T_{y})j)^{2} + \cdots + ((C_{y} - T_{y})i - (C_{y} - T_{y})j)^{2} + \cdots + ((C_{y} - T_{y})i - (C_{y} - T_{y})j)^{2} + \cdots + ((C_{y} - T_{y})i - (C_{y} - T_{y})j)^{2} + \cdots + ((C_{y} - T_{y})i - (C_{y} - T_{y})j)^{2} + \cdots + ((C_{y} - T_{y})i - (C_{y} - T_{y})j)^{2} + \cdots + ((C_{y} - T_{y})i - (C_{y} - T_{y})j)^{2} + \cdots + ((C_{y} - T_{y})i - (C_{y} - T_{y})j)^{2} + \cdots + ((C_{y} - T_{y})i - (C_{y} - T_{y})j)^{2} + \cdots + ((C_{y} - T_{y})i - (C_{y} - T_{y})j)^{2} + \cdots + ((C_{y} - T_{y})i - (C_{y} - T_{y})j)^{2} + \cdots + ((C_{y} - T_{y})i - (C_{y} - T_{y})j)^{$$

given in terms of the 9 parameters output from CAM. Each CATIA program included PPWords to specify the parameters required for constant surface speed calculations for input into the post processor that are not otherwise output from CAM in the APTSource file.

The following parameters are required for the constant surface speed calculation to output the variable spindle speed and feedrate values on each line of the NC code where the cutter is in contact with the component.

- 1. Desired Constant Surface Speed, Vc, in m/min.
- 2. Desired Constant Feed per Tooth, fz, in mm.
- 3. Number of cutting edges, Z.

With these parameters specified, the Spindle Speed, S, in RPM and linear feedrate, F, can now be calculated for the effective diameter at each contact point.

$$S = \frac{1000V_c}{\pi D_{eff}} \tag{2}$$

$$F = fz \cdot S \cdot Z \tag{3}$$

The calculations for constant maximum chip thickness require the following additional parameters to be specified:

- Desired Constant Maximum Chip Thickness.
- Radial cutting depth.
- Bottom radius of the conical tapered barrel mill.
- Barrel radius of the conical tapered barrel mill.
- Top/neck radius of the conical tapered barrel mill.
- Barrel radius angle of the conical tapered barrel mill.
- Conical tapered barrel mill tool diameter.

These parameters allow the chip thinning effects of the barrel angle at the point of contact to be considered so that a feedrate can be calculated that will maintain a constant maximum chip thickness as the contact point varies rather than a constant feed per tooth.

The details of this calculation are too lengthy to include here and will be included in a later journal paper.

3 EXPERIMENTAL TRIALS

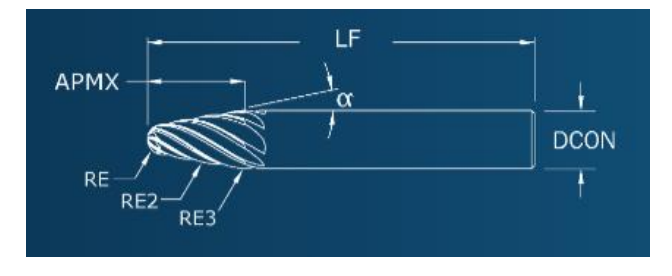
The proposed method has been tested on 3 different 5-axis machine tools, namely the Hermle C52, DMG Mori Lasertec 85 and Cincinatti H5. Each with different kinematic configurations. For brevity, the authors present the experimental results from the Hermle C52 noting that results across all platforms were similar.

Note - Prior to conducting variable RPM operations on a Siemens 840D controlled machine tool, the NC parameters in Table A1 are required to be changed followed by a Numerical Controller Kernel (NCK) reset.

3.1 TOOLING

A CTB milling tool was used for the testing. Figure 4 shows the geometry of the CTB milling tool and Table 1 shows the associated geometry parameters for the SGS45717 8 Flute TH Coated Tapered End Mill.

Fig. 4: CTB Milling Tool Geometry



Tab. 1: CTB Milling Tool Geometry parameters

Parameter	Value
Shank diameter DCON (mm)	16
Length of cut APMX (mm)	8.5
Overall Length LF (mm)	109
α	20
RE (mm)	3
RE2 (mm)	60
RE3 (mm)	5
# Teeth	8

3.2 Experimental Testing

A range of tests were conducted to determine the impact of:

- 1. CAM settings (CL discritisation)
- 2. Machine tool controller settings
- 3. Spindle drive limits
- 4. Machine tool limits.

For brevity, the authors present results from 3 of the case studies, which includes two successful trials and an unsuccessful trial to demonstrate there are more factors at play than purely kinematic control to determine the successful implementation of the proposed method. For the first two results, the A-axis controls the kinematic transformation and the third is controlled by the C-axis.

The tests are all straight line tests where the engagement along the CTB tool changes throughout the cut as shown in Figure 5.

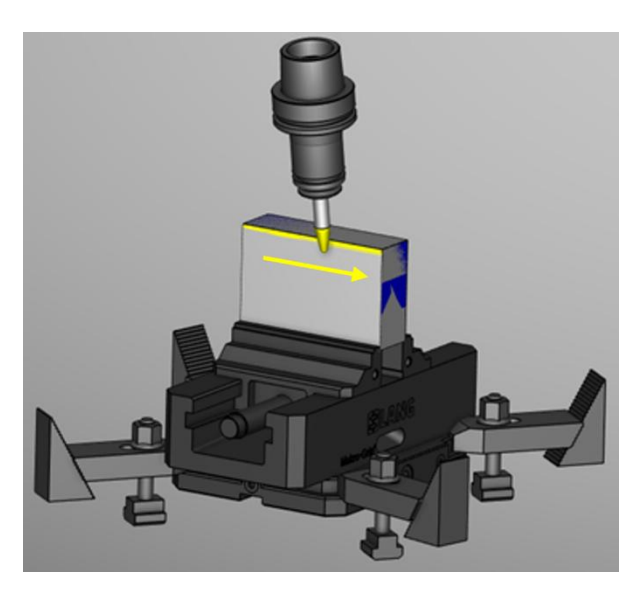
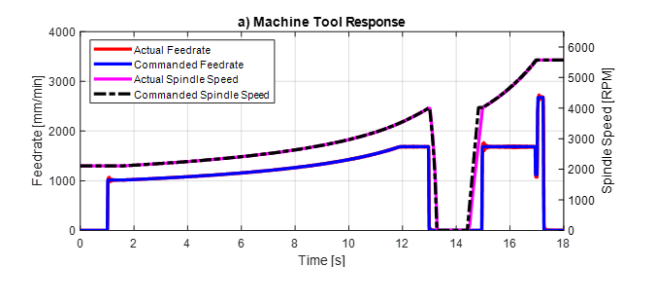


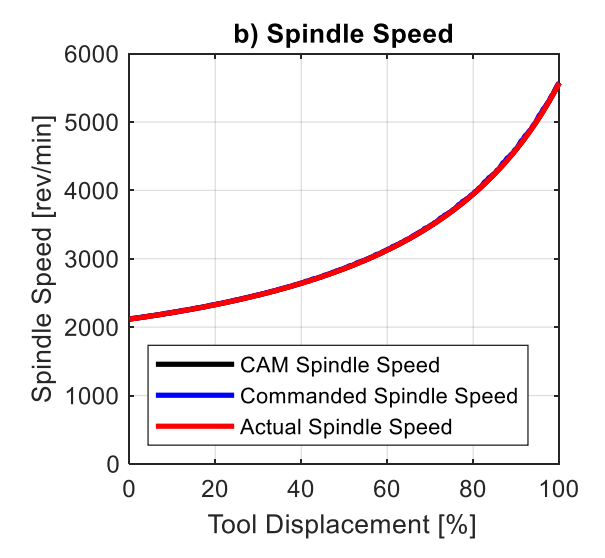
Fig. 5: Straight line test

3.3 A-Axis Controlled - Successful Test

The first part program has a CAM tolerance of 10 μ m, A-axis controlled motion and is designed with a constant FPT of 0.06 mm. The machining parameters are included in Table A2.

Figure 6 a,b and c show that there is no deviation from the CAM spindle speed and feedrate commands with the NC commanded and actual spindle speed and feedrate. The spindle speed and feedrate both drop to zero when the spindle speed crosses 4000 RPM. This is likely due to the change between the low and high speed spindle windings. These parameters are suitable for CTB milling with the constraint of a maximum 4000 RPM spindle speed.





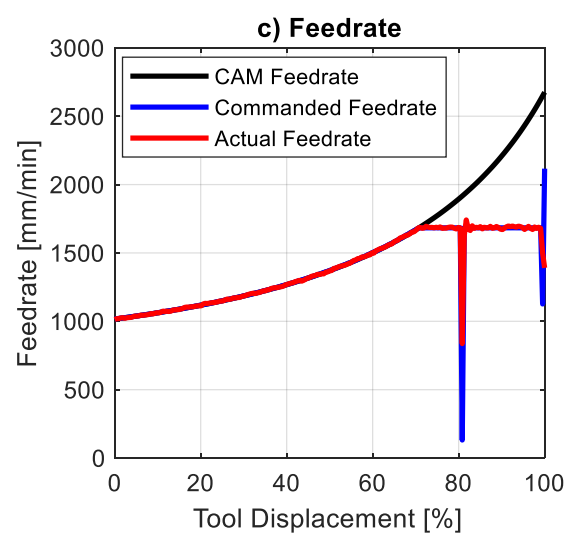
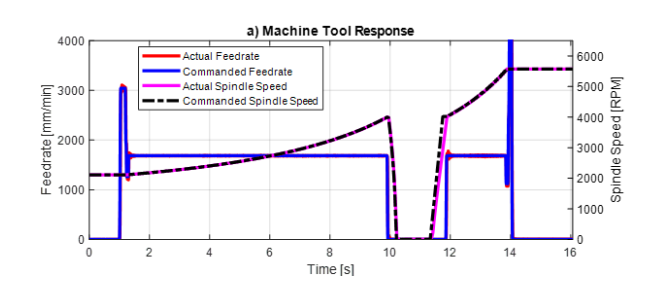


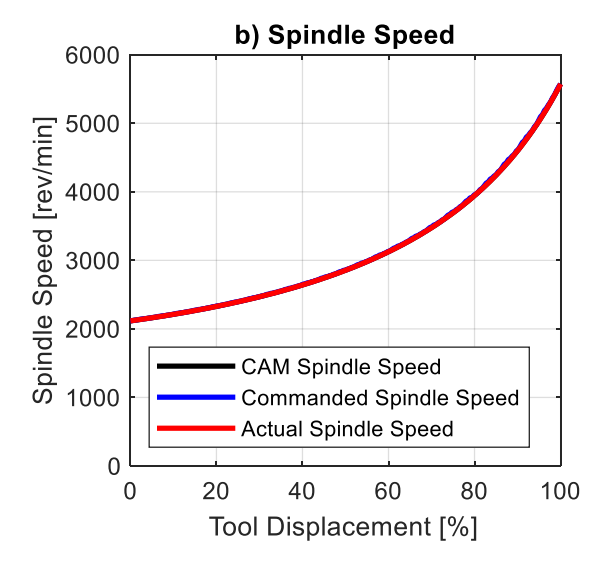
Fig. 6: A-Axis controlled -successful test results

3.4 A-Axis Controlled - Unsuccessful Test

The part program has a CAM tolerance of 10 μ m, A-axis controlled motion and is designed with a constant FPT of 0.18 mm. The machining parameters are included in Table A2

Figure 7 a,b and c show that there is no deviation from the CAM spindle speed and feedrate commands with the NC commanded and actual spindle speed and feedrate. However, despite the spindle speed control performing as expected, the feedrate did not achieve the required CAM feedrate. As can be seen in Figure 7a and 7c, the commanded feedrate is stalled and so the actual feedrate is never commanded to reach the CAM feedrate. This is an issue with the NC interpolator behaviour and not the kinematic limitations of the machine tool.





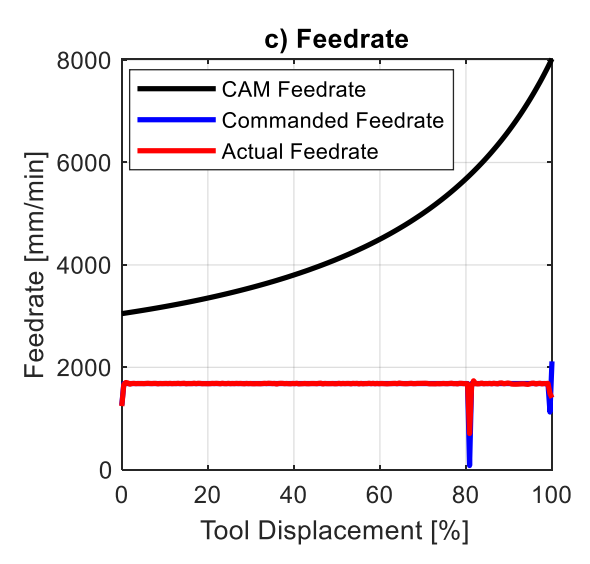


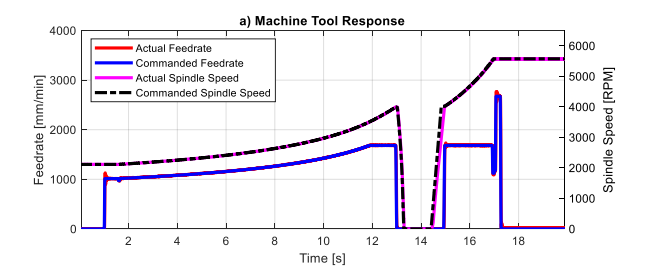
Fig. 7: A-Axis controlled -unsuccessful test results

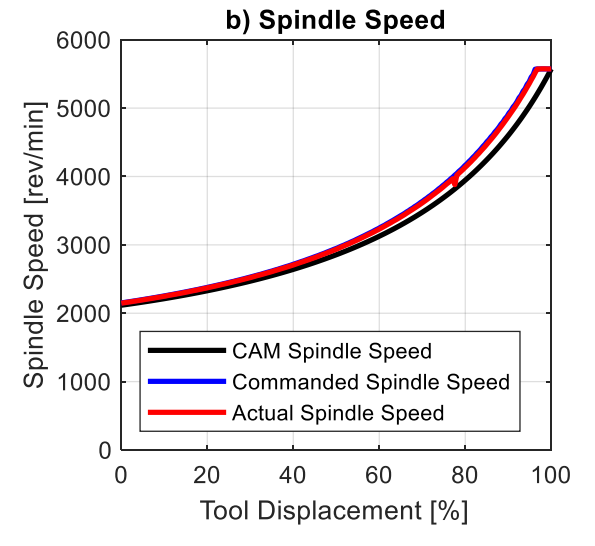
3.5 C-Axis Controlled - Successful Test

To prove the variability of method with different controlled axis configurations on the same machine tool, in this test the authors fixed the A-axis and used the C-axis to control the motion. The machining parameters are included in Table 2.

The part program has a CAM tolerance of 10 μ m, fixed A-axis and C-Axis controlled motion and is designed with a constant FPT of 0.06 mm.

Figures 8a,b and c show that there is minor deviation from the CAM spindle speed and feedrate commands with the NC commanded and actual spindle speed and feedrate. More investigation is required to determine the root cause. However, it was proven that the C-axis controlled configuration is feasible for variable CTB spindle speed operations.





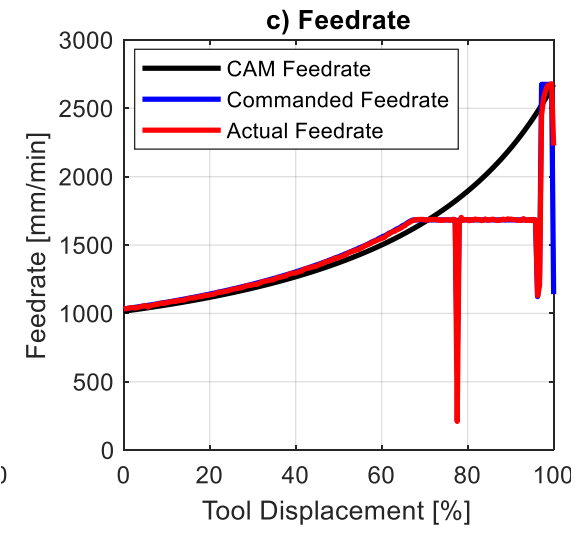


Fig. 8: C-Axis controlled -successful test results

4 DISCUSSION

The results show that it is possible to vary both the spindle speed and feedrate during CTB milling operations. However, it has been noted there can be unwanted behaviours in the spindle speed and feedrate responses caused by numerous factors which include:

- 1. CAM settings (CL discritisation)
- 2. Machine tool controller settings
- 3. Spindle drive limits
- 4. Machine tool limits.

The authors noted from programs with fine CAM tolerances that feedrate limitations occur but the spindle speed remains largely unaffected.

The authors also highlight there is a requirement to modify the Siemens 840D NC settings. If these settings are not

modified then the smooth continuous motion of the spindle speed modulation and feedrate scheduling will not occur. No CAM or virtual machining software can detect this issue.

The kinematic limits of the Cartesian and rotary feed drives are unlikely to be a limiting factor in the application of varying spindle speed on-the-fly for CTB milling operations.

There are other constraints such as the interpolator and spindle kinematics which may prevent the one-to-one mapping from the CAM commands to actual feedrate and spindle speed outputs.

5 SUMMARY

The following conclusions can be drawn from the project:

- The ability to perform variable RPM CTB milling operations was successfully demonstrated.
- A new capability was developed to output the necessary format to control the spindle speed of the tool whilst the tool tangency point is moving across the barrel radius using the AMRC in-house post-processer and CATIA.
- The requirements and limitations of a machine tool and associated controller to perform variable RPM CTB milling operations were investigated and a set of parameters and settings defined to enable the motion capability.
- 4. The effect of resolution on parameter changes was investigated and it was discovered that there are unwanted behaviours in the spindle speed and feedrate responses caused by numerous factors which include CAM settings, machine tool controller settings and spindle drive limits. These behaviours are not predicted by CAD/CAM or virtual machining simulations and therefore warrant further investigation.

Future work will apply this method, with the constraints identified, to both 5-axis machining of a medical knee implant and an aeroengine blisk.

This work was supported by HVM Catapult funding provided by Innovate UK.

6 ACKNOWLEDGMENTS

7 REFERENCES

[Lu 2019] Lu, Y. A., Ding, Y., Wang, C. and Zhu, L. Tool path generation for five-axis machining of blisks with barrel cutters. International Journal of Production Research, 2019, 57, 5.

[Luo 2016] Luo, M., Yan, D., Wu, B. and Zhang, D. Barrel cutter design and toolpath planning for high-efficiency machining of freeform surface. International Journal of Advanced Manufacturing Technology, 2016, 85, 9–12.

[Meng 2014] Meng, F. J., Chen, Z. T., Xu, R. F. and Li, X. Optimal barrel cutter selection for the CNC machining of blisk. CAD Computer Aided Design, 2014, 53.

[Reznicek 2025] Reznicek, M., Horava, C. and Ovsik, M. Evaluation of Cutting Forces and Roughness During Machining of Spherical Surfaces with Barrel Cutters. Materials, 2025, 18, 15, 3630.

[Suzuki 2021] Suzuki, T., Okamoto, K. and Morishige, K. Tool path generation for five-axis controlled machining of free-form surfaces using a barrel tool considering continuity of tool postures. International Journal of Automation Technology, 2021, 15, 6, 885–892.

[Vavruska 2023] Vavruska, P., Bartos, F., Stejskal, M., Pesice, M., Zeman, P. and Heinrich, P. Increasing tool life and machining performance by dynamic spindle speed control along toolpaths for milling complex shape parts. Journal of Manufacturing Processes, 2023, 99, 283–297.

Tab. A1: CTB Milling Tool Geometry parameters

Parameter	Action
MC_AUXFU_M_SYNC_TYPE	0 to 1
MC_AUXFU_S_SYNC_TYPE	0 to 3
SPIND_ON_SPEED_AT_IPO_START	0 to 1

Tab. A2: Machining parameters

Program Description	Flutes	Ae (mm)	Vc (m/min)	FPT (mm)	CYCLE832	CAM Tol (mm)
C-Axis Controlled – Successful	8	0.7	104	0.06	0.1 ROUGH	0.01
C-Axis Controlled – Unsuccessful	8	0.7	104	0.18	0.1 ROUGH	0.01
A-Axis Controlled – Successful	8	0.7	104	0.06	0.1 ROUGH	0.01